Journal of Structural Chemistry. Vol. 58, No. 7, pp. 1403-1410, 2017.

IN SITU ANALYSIS OF THE FORMATION STEPS OF GOLD NANOPARTICLES BY OLEYLAMINE REDUCTION

M. V. Kirichkov[1], A. A. Guda[1], A. P. Budnyk[1], T. A. Lastovina[1], A. L. Bugaev[1], V. V. Shapovalov[1], Yu. V. Rusalev[1], A. V. Chernyshev[2], and A. V. Soldatov[1]

UDC 544.77.051.5:544.77.022

A colloidal solution of gold nanoparticles is synthesized with the use of sodium tetrachloroaurate(III) as a precursor, oleylamine as a reducer and surfactant, and 1-octadecene as a solvent. Reaction stages are analyzed *in situ* by optical (UV-vis) absorption spectroscopy with a simultaneous analysis of particle sizes by dynamic light scattering and X-ray absorption near edge spectroscopy for the analysis of the gold oxidation state. After the synthesis the size of obtained nanoparticles is determined by transmission electron microscopy. The analysis of the obtained experimental data reveals the presence of three main steps in the reduction reaction mechanism, corresponding to Au^{3+}, Au^{+}, Au^{0}, which enables the construction of the reaction model. The reaction mechanism involves the formation of gold(I) complexes with oleylamine, followed by polymerization and the formation of gold nanoclusters coated with oleylamine.

DOI: 10.1134/S0022476617070186

Keywords: TEM, DLS, XANES spectroscopy, UV-vis, gold nanoparticles, oleylamine.

INTRODUCTION

Metallic nanoparticles (NPs) play an important role in many modern technologies for biomedicine [1], catalysis [2, 3], fuel cell manufacture [4], data storage [5], and solar cells [6]. Owing to their great application potential in optoelectronics [7], catalysis [8], and biotechnologies [9], gold NPs have been most intensely studied. Gold NPs are usually grown on a substrate [10] or a solution [11]; the obtained particles can have different shapes, size distributions, and degrees of aggregation. Under illumination a plasmon resonance arises on the surface of gold NPs, which is manifested as characteristic absorption in the green range of the optical spectrum of NPs [12].

The most popular synthesis techniques are the reduction of gold halides by various reducers. The NP synthesis process can be divided into four main steps: nucleation (1), coalescence of obtained NPs into larger ones (2), particle growth (3), rapid growth of NPs to the full end of the gold precursor (4). The nucleation rate depends on the reagent concentrations and also on the chemical nature of the reducer [13].

One of the easiest and most efficient techniques to obtain colloidal gold consists in the reduction of gold(III) from $HAuCl_4$ or $NaAuCl_4$ by means of citrates (e.g., from $Na_3C_6H_5O_7$) in water. For the first time, this synthesis was

[1]International Research Center "Smart Materials", Southern Federal University, Rostov-on-Don, Russia; mikhail.kirichkov@gmail.com. [2]Institute of Physical and Organic Chemistry, Southern Federal University, Rostov-on-Don, Russia. Translated from *Zhurnal Strukturnoi Khimii*, Vol. 58, No. 7, pp. 1442-1449, September-October, 2017. Original article submitted December 30, 2016; revised February 16, 2017.

systematically performed in 1951 by J. Turkevich to study the NP nucleation and growth processes [10]. This synthesis technique was named after him, and the extended version has been known as the Turkevich–Frens method [15].

Another well-known method of synthesizing NPs is a rapid reduction of gold(III) salt with the use of sodium tetrahydroborate ($NaBH_4$) in an aqueous medium [16]. In this method three main steps can be distinguished. The first step is characterized by coalescence processes in which the total number of NPs decreases but their mass fraction remains constant. At the second step, NPs continue to grow to an average size of 5 nm, with the number of particles remaining constant here. The final step of the synthesis consists in a rapid reduction of the remaining precursor, which causes an abrupt increase in the particle size and a decrease in their polydispersion to 10%. The use of tetrahydroborates is an efficient method of obtaining metal NPs in any aqueous medium (acidic, neutral, basic). Here the reducing activity of tetrahydroborates increases with increasing acidity of the solution, which is due to the accelerated hydrolysis of the BH_4^- ion that is accompanied by the appearance of intermediate hydrated forms (BH_2OH, $BH(OH)_2$, BH_3OH^-, etc.) being stronger reducers than BH_4^- [17]. A disadvantage of the method is a possible formation of elementary boron which is catalyzed by gold NPs formed and is accompanied by its incorporation into the structure of the metal particle [17].

The third popular method of obtaining colloidal gold consists in the application of sodium tetrachloroaurate(III) as a gold precursor, citric acid ($C_6H_8O_7$) as a reducer, and polyvinylpyrrolidone as a stabilizer of NPs [18]. As the previous one, this synthesis consists of three main steps. The first step is the formation of Au_2Cl_6 dimers that, at the second step, form small gold nanoclusters, e.g. Au_{13}. At the third step, large clusters grow through coalescence processes [19].

It is necessary to understand the formation and growth mechanism of NPs during the synthesis to control the size and shape of the obtained particles. The diversity of factors affecting the reaction, the dynamic character of systems under study, experimental difficulties in data measurements retain the controversial character of the available data on the mechanisms of the above popular synthesis methods of gold NPs.

In this work, we turned to the known technique of obtaining gold NPs in the organic medium with the use of oleylamine (OAm, $C_{18}H_{35}NH_2$) as a reducer [9]. Oleylamine has been widely applied in the synthesis of metal or metal oxide NPs [20, 21]. Its amino group can act as an electron donor with increasing temperature, and a long hydrocarbon chain enables the stabilization of obtained NPs [22]. A long-term contact between oleylamine and the gold precursor leads to the formation of gold nanofibers/nanowires already at room temperature [23]. Gold obtained with the use of oleylamine has the hydrophobic surface and can be easily transferred into a colloidal solution in hexane or chloroform [23]. Moreover, the introduction of a polar solvent during the synthesis provides the complete or partial formation of NPs instead of nanofibers [24]. In the mentioned work it is assumed that the formation energy of $Au(0)\cdots NH_2R$ and $Au(I)\cdots NH_2R$ bonds is about 44 kJ/mol and is comparable with the formation energy of $C_2H_5OH\cdots NH_2R$ hydrogen bonds (5-30 kJ/mol), which can cause the breakage of oleylamine chains.

The anisotropy of the product growth in the solution suggests that the structural features of a reducer-stabilizer molecule play a significant role. The introduction of an additional solvent can affect the growth mechanism as well as the microstructural characteristics of gold NPs obtained with the use of oleylamine.

We have synthesized gold NPs by the oleylamine reduction of sodium tetrachloroaurate(III) in the 1-octadecene ($C_{18}H_{36}$) medium. The obtained spherical NPs had sizes ranging from 6 nm to 15 nm with an average radius of 10 nm. The synthesis process was controlled *in situ* by spectral techniques, which made it possible to distinguish the main steps in the NP formation. We used the data collected by the techniques such as optical absorption spectroscopy, dynamic light scattering to analyze NP sizes, XANES, and transmission electron microscopy (TEM). Furthermore, the analysis by UV-vis and DLS techniques was performed simultaneously and on the same sample, which became possible due to the application of the elaborated heating cell.

EXPERIMENTAL

The reaction mixture for the synthesis of the colloidal solution of gold NPs was prepared according to [9]. In a glass beak on a magnetic stirrer 4 ml of 1-octadecene, 0.4 ml of oleylamine, and 0.02 g of sodium tetrachloroaurate(III) were mixed. All reagents (Sigma-Aldrich) were analytically pure.

For the *in situ* analysis by UV-vis and DLS techniques the reaction mixture was poured into the standard quartz cuvette with an optical path length of 10 mm. During the experiment the cuvette was fixed between two parallel planar heating elements. These elements were mounted on a single chassis and placed inside the measurement chamber of the spectrophotometer. They provided the simultaneous heating of two cells with the sample under study and the reference sample. Pure 1-octadecene was taken as the reference sample. The temperature of the reaction mixture was maintained at 80 °C; the synthesis duration was 120 min. After this the reaction mixture was cooled to room temperature, twice washed with a mixture of water and ethanol in the 1:1 ratio, and the precipitate was dispersed in hexane C_6H_{12}.

For the measurement of UV-vis spectra a double-beam SHIMADZU UV-2600 spectrophotometer was used. The measurement time of one spectrum in the range 190-900 nm was 67 c; in total, 140 measurements were performed.

To the cuvette with the sample being studied an optical probe of a Microtrac Nano-flex analyzer of NP sizes was dipped (not overlapping the spectrophotometer beam). A laser with a wavelength of 780 nm was employed. The acquisition time for the single particle distribution in the solution was 90 s; in total, 90 distributions were obtained. The signal of the background (oleylamine + 1-octadecene in the 1:10 ratio) was preliminary measured for 360 s, which made it possible to exclude the oleylamine dispersion from the analysis of the size distribution.

The gold oxidation state was characterized by XANES on a BM01b Swiss-Norwegian beamline at the European Synchrotron Radiation Facility (ESRF). The solution of the sample was placed in a capillary with a diameter of 2 mm, which was heated by an air heater. The X-ray beam size was 1 mm wide and 0.3 mm high. The absorption spectra were measured in transmission mode by means of a Si(111) monochromator in continuous scanning mode. Gold foil was inserted between the second and third ionization chambers to calibrate the energy positions of the spectra.

The TEM analysis was carried out on a Tecnai G2 Spirit BioTWIN microscope with an accelerating voltage of 120 kV.

RESULTS AND DISCUSSION

During the synthesis of gold NPs a change in the color of the reaction mixture is observed, which can be divided into two stages. The first stage involves a transition from the initial orange color to yellow with subsequent discoloration until full transparency of the solution. The second stage is characterized by a gradual appearance of the red color in the reaction mixture until a wine-red color. The optical absorption spectra (Fig. 1) are correspondingly divided into two groups. At the first stage, the absorption curve gradually shifts to the left and declines, which corresponds to a total decrease in the absorbance in the visible range and discoloration of the solution. At the second stage, the appearance and growth of the plasmon resonance peak at 520 nm is observed, which is manifested as reddening of the solution.

To analyze a series of optical absorption spectra, for each of them the ratio was calculated between the absorbance values on the surface plasmon resonance peak and the value at 450 nm. As shown in [25], this ratio correlates with a size of small gold NPs, and hence, enables the study of the dynamics of changes in their sizes during the synthesis. The data obtained evidence a gradual increase in NP sizes when the solution becomes red. The final values of NP sizes are within 8-12 nm.

DLS measurements were performed simultaneously with the UV-vis measurements. The size distribution data show two main steps in the process. The first step, corresponding to solution discoloration according to the optical absorption results, is characterized by a weak signal from larger (~0.5 μm) particles. The second step, corresponding to reddening of the solution in the UV-vis analysis, is characterized by a strong signal from 8-12 nm gold NPs formed.

In Fig. 2 both synthesis stages distinguished in the DLS data can be observed. An abrupt transition from the distribution corresponding to large particles to a narrow distribution for small NPs can be noted. When the second phase

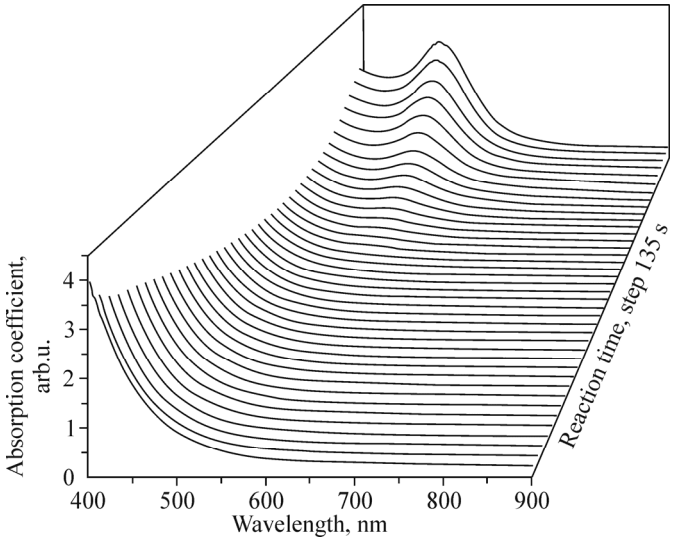

Fig. 1. Optical absorption spectra of the reaction mixture during the reaction.

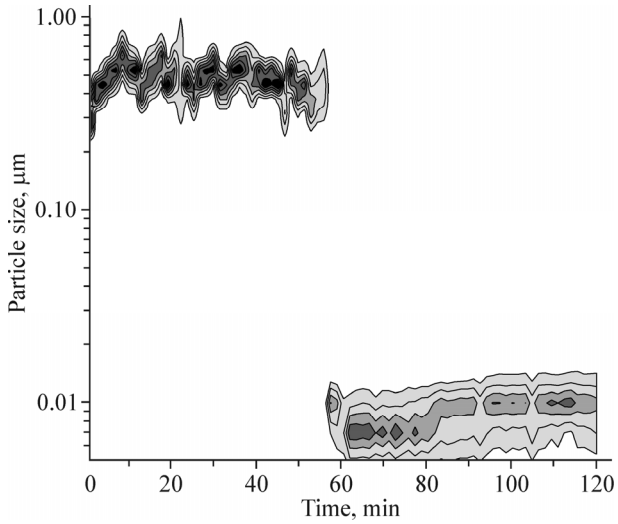

Fig. 2. *In situ* DLS characterization during the reaction. An abrupt transition between two synthesis stages is noticeable (different black colors show the DLS signal intensity; a darker color corresponds to the increasing signal).

appears, the distribution maximum is at ~8 nm, and then shifts to larger sizes of 10-12 nm, which corresponds to the growth of gold NPs. The occurrence of a transition region of the co-existence of both distributions, which corresponds to the onset of the NP nucleation process, is noteworthy.

The X-ray absorption spectra were measured every 3 min in transmission mode, as shown in Fig. 3.

The data obtained (only one of every three spectra is shown) after the subtraction of the background and normalization are given in Fig. 4. During the first 10 min of the reaction an abrupt decrease in the white line intensity occurs at an energy of 11920 eV, which indicates a decrease in the gold oxidation state. Then the absorption spectral shape slowly changes, evidencing a change in the local atomic structure near the gold atoms. The positions of peaks in the X-ray absorption spectrum at the final stage of the process allow the assumption of the formation of small metal NPs in the reaction course.

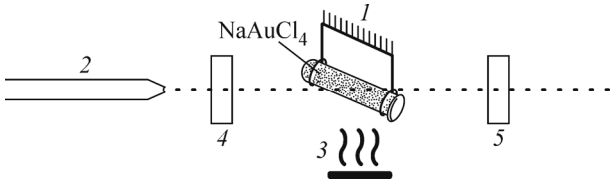

Fig. 3. Scheme of the experimental instrument for measuring XANES spectra: capillary with the solution (*1*), X-ray source (*2*), heater (*3*), input and output detectors (*4* and *5*).

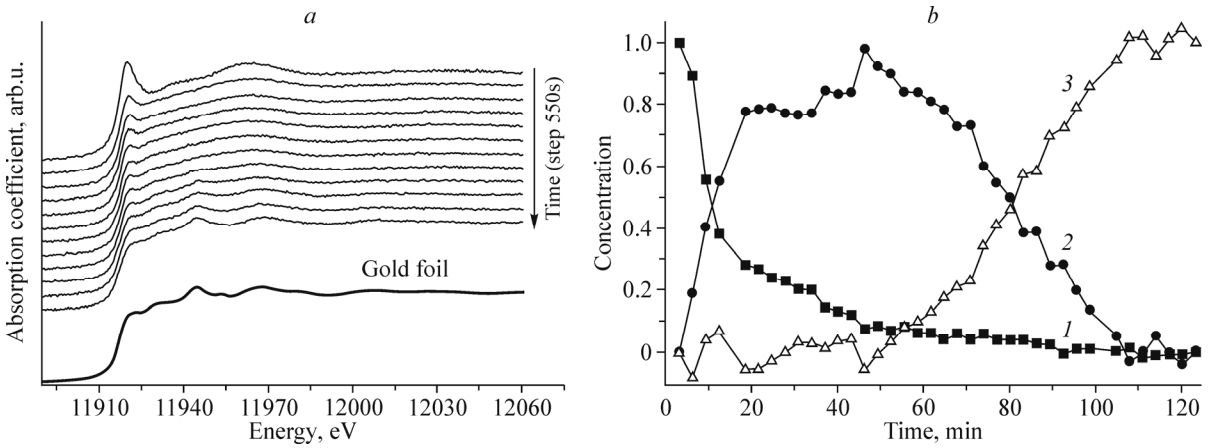

Fig. 4. Gold L_3-edge XANES spectra of the reaction mixture heated to 80 °C, in every 550 s (*a*) and a change in the molar fractions of three main components during the reaction for a series of spectra from Fig. 4*a*, where Au^{3+} (*1*), Au^{1+} (*2*), Au^0 (*3*) (*b*).

For the quantitative analysis of the obtained X-ray spectral data we applied a mathematical procedure to a series of XANES spectra (the analysis of main components) [26, 27]. Statistical criteria indicate the presence of three independent components in the series of the spectra. Therefore, the spectral matrix was fitted by three independent components and for the solution to be unambiguous the restrictions were imposed: the concentrations of these components must be non-negative and vary from 0 to 1, and also the first and last spectra were true, i.e. the molar fraction of two of the three components was 0. The molar fractions obtained are shown in Fig. 4*b*. In the time dependences of the molar fractions of the components a rapid transition from the initial Au^{3+} state to the intermediate Au^{1+} phase can be observed during the first 20 min of the reaction, which is replaced by a slow formation of the third phase: Au^0 NPs.

The obtained colloidal solution of gold NPs kept for 120 min at a temperature of 80 °C was analyzed by TEM (Fig. 5*a*). It can be seen that most particles have a spherical shape and large agglomerates are absent.

From the analysis of several these images (in total, about 300 NPs were examined), the NP size distribution was obtained (Fig. 5*b*). The distribution shows that most particles have sizes in the range 8-10 nm.

Based on the data obtained from the *in situ* analysis in this work and the literature [28-30] a scheme of the reaction mechanism in this synthesis was constructed. The synthesis consists of three stages. The initial time moment corresponds to Au^{3+} gold ions. At the initial stage, the Au^{3+} gold complexes are bonded to chlorine atoms and the oleylamine molecule is in the outer sphere, substituting for sodium in the structural formula of the initial $NaAuCl_4$ salt. Due to thermolysis resulting from heating the reaction mixture, Au^{3+} is reduced to Au^+, and AuCl(oleylamine) complexes form (Fig. 6*a*). The AuCl(oleylamine) complexes are stable and sufficiently slowly decompose, which provides the better control of the particle growth [22]. In [31] it is also noted that the surface of golda Au^0 NPs formed can absorb $AuCl_4^-$ ions and amine molecules

$$[Au_n^0(AuCl_4^-)_m](aq) + mRNH_3^+(org) \rightarrow [Au_n^0(AuCl_4^-)_m](RNH_3^+)_m(org),$$

where org is the organic medium. Similarly, Au(I) gold can participate in the complexation

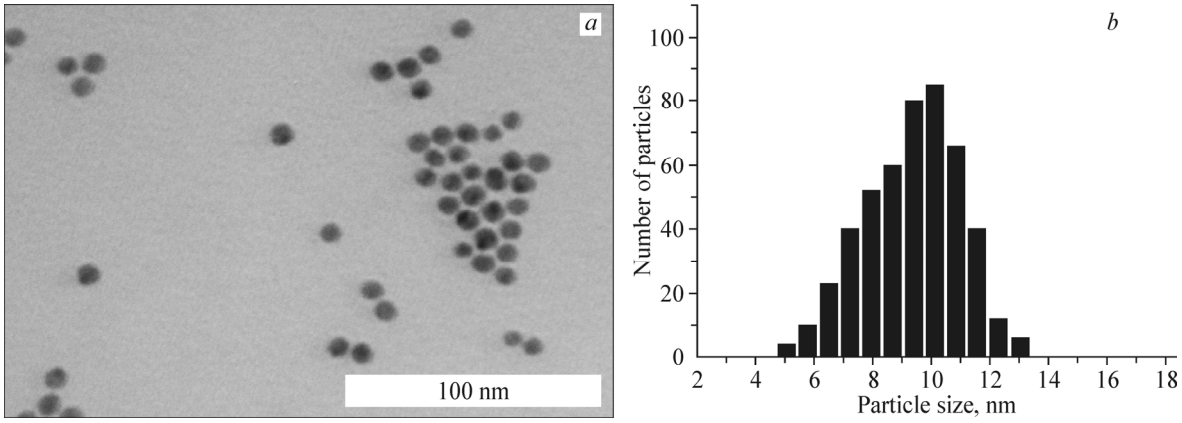

Fig. 5. TEM image of gold NPs (*a*) and size distribution based on the analysis of several such images (*b*).

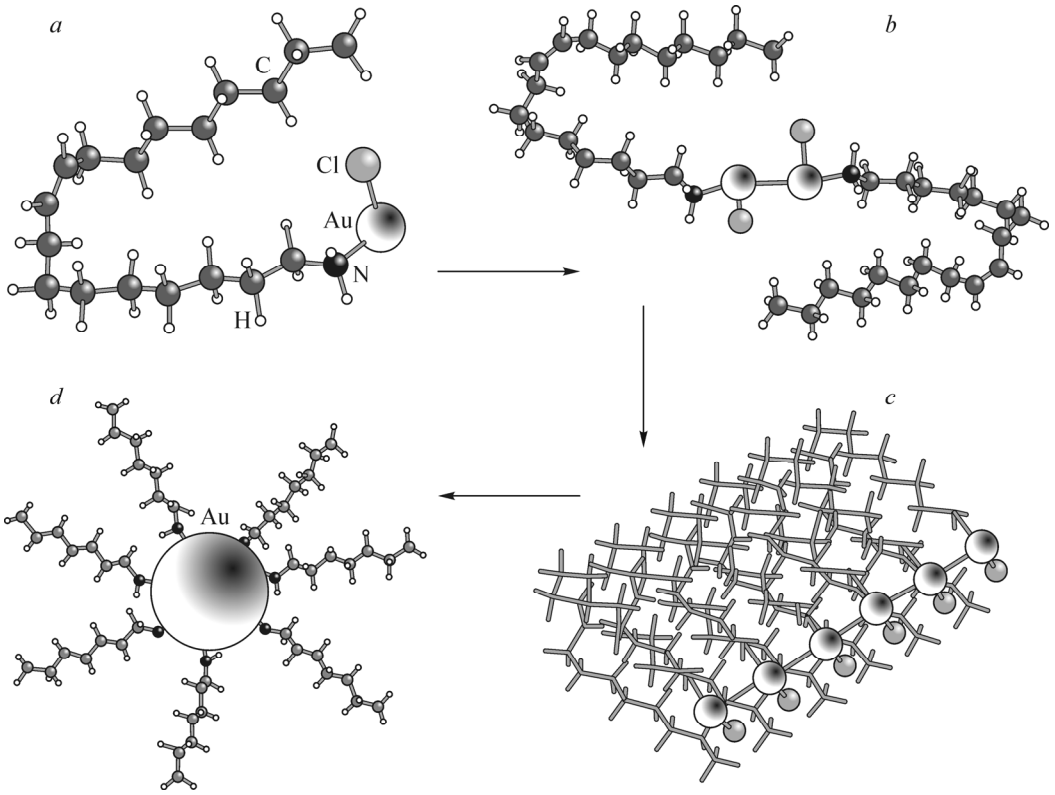

Fig. 6. Scheme of the reaction mechanism: complexation: formation of the AuCl(Oleylamine) complexes (*a*), formation of dimers/trimers (*b*), formation of long 1D chains from them (*c*), and final formation of the gold nanocluster (*d*).

$$[Au_n^0(AuCl_2^-)_m](aq) + mRNH_3^+(org) \rightarrow Au_n^0[AuCl(RNH_2)]_m(org) + HCl,$$

where aq is the aqueous medium. The complex formed is stable and decomposes sufficiently slowly.

Owing to a strong non-covalent interaction of the Au(I)–Au(I) type, the AuCl(oleylamine) complexes formed at the first stage are involved in the formation of dimers [32] or even larger aggregates (Fig. 6*b*, *c*). The authors of [18] suggest that long one-dimensional (1D) polymer chains rapidly form from $[AuCl(oleylamine)]_2$ dimers (Fig. 6*c*). The appearance of these chains is attributed to linear coordination. The introduction of 1-octadecene seem to facilitate the breakage of chains formed by AuCl(oleylamine) complexes due to hydrophobic interactions. It should also be noted that at the selected synthesis temperature the disproportionation of the gold(I) complex to Au(0) and Au(III) is not observed.

When large aggregates are formed from AuCl(oleylamine) complexes, gold NPs also form, which is promoted by a close location of gold atoms in the aggregates. During the natural coagulation process the core composed of gold atoms becomes surrounded by oleylamine chains (Fig. 6*d*). It should be noted that gold nanoclusters grow gradually, which is confirmed by a shift of the peak in Fig. 2 and gradual growth of the plasmon resonance peak in Fig. 1.

CONCLUSIONS

The work presents a complex analysis of the synthesis of the colloidal solution of gold NPs during the reduction of sodium tetrachloroaurate(III) with oleylamine and the use of 1-octadecene as the solvent. DLS, UV-vis, and gold L_3-edge XANES techniques were employed for characterization. The obtained colloidal solution was analyzed by TEM. The application of the specially constructed heating cell enabled the simultaneous characterization by UV-vis and DLS techniques.

The experimental data obtained allowed us to distinguish three main stages in the synthesis of colloidal gold. Thus, the analysis by UV-vis optical absorption spectroscopy clearly shows a decrease in the absorption coefficient during solution discoloration from 3 to 1.5 and the appearance of the plasmon resonance peak at 520 nm when its color changes. The analysis of the plasmon resonance peak position and amplitude indicates the gradual growth of gold NPs. By DLS the particle size distribution in the reaction mixture was constructed during the synthesis, which reveals an abrupt transition from 0.5 μm particles to particles with sizes of 6-8 nm along with the appearance of the plasmon resonance peak in the optical absorption spectra. Later on, particle sizes increase to 10-12 nm, which is accompanied by the respective shift of the distribution peak. The numerical analysis of the X-ray absorption spectra reveals the occurrence of three main stages in the synthesis that differ in the gold oxidation state (Au^{3+}, Au^{1+}, and Au^0), along with a change in the concentrations of these components during the synthesis. Thus, on the first stage of the reaction, a rapid transition from Au^{3+} to Au^{1+} occurs followed by slow reduction of Au^{1+} to metallic gold is observed. The reaction products were studied by TEM that shows a narrow distribution of obtained NPs with a maximum near 10 nm.

The work was supported by the garnt “Computer Nanodesign, Synthesis, and Diagnostics of Quantum Nanostructures” of the Ministry of Education and Science of the Russian Federation, the project part of State Contract No. 16.148.2014/K and the Grant of the President of the Russian Federation for young scientists MK-7300.2016.2.

REFERENCES

1. Q. A. Pankhurst, N. T. K. Thanh, S. K. Jones, and J. Dobson, *J. Phys. D: Appl. Phys.*, **42**, 224001 (2009).
2. D. Astruc, F. Lu., and J. R. Aranzaes, *Angew. Chem., Int. Ed.*, **44**, 7852 (2005).
3. R. Narayanan and M. A. El-Sayed, *J. Phys. Chem. B*, **109**, 12663 (2005).
4. H. Bonnemann and R. Richards, *Europ. J. Inorg. Chem.*, **10**, 2455 (2001).
5. T. Hyeon, *Chem. Commun.*, **8**, 927 (2003).
6. H. A. Atwater and A. Polman, *Nat Mater.*, **9**, 205 (2010).
7. M. Treguer-Delapierre, F. Rocco, G. Lelong, A. Le Nestour, T. Cardinal, A. Maali, and B. Lounis, *Solid State Sci.*, **7**, 812 (2005).
8. B. Hvolbæk, T. V. W. Janssens, B. S. Clausen, H. Falsig, C. H. Christensen, and J. K. Norskov, *Nano Today*, **2**, 14 (2007).
9. M. Wang, C. Wang, K. L. Young, L. L. Hao, M. Medved, T. Rajh, H. C. Fry, L. Y. Zhu, G. S. Karczmar, J. S. Jiang, N. M. Marcovic, and V. R. Stamencovic, *Chem. Mater.*, **24**, 2423 (2012).
10. Y. Jin, X. F. Kang, Y. H. Song, B. L. Zhang, G. J. Cheng, and S. J. Dong, *Analyt. Chem.*, **73**, 2843 (2001).
11. T. K. Sau and C. J. Murphy, *J. Am. Chem. Soc.*, **126**, 8648 (2004).
12. I. H. El-Sayed, X. H. Huang, and M. A. El-Sayed, *Nano Lett.*, **5**, 829 (2005).
13. L. A. Dykman and V. A. Bogatyrev, *Usp. Khim.*, **76**, No. 2, 199 (2007).

14. J. Turkevich, P. C. Stevenson, and J. Hillier, *Discuss. Faraday Soc.*, **11**, 55 (1951).
15. K. Zabetakis, W. E. Ghann, S. Kumar, and M. C. Daniel, *Gold Bull.*, **45**, 203 (2012).
16. P. Jörg, K. Ralph, R. Martin, R. Uwe, R. Heinrich, F. T. Andreas, and E. Franziska, *J. Phys.: Conf. Ser.*, **247**, 012051 (2010).
17. A. D. Pomogailo, A. S. Rosenberg, and I. E. Uflyand, *Khimiya* [in Russian], Moscow (2000).
18. N. T. K. Thanh, N. Maclean, and S. Mahiddine, *Chem. Rev.*, **114**, 7610 (2014).
19. T. Yao, Z. H. Sun, Y. Y. Li, Z. Y. Pan, H. Wei, Y. Xie, M. Nomura, Y. Niwa, W. S. Yan, Z. Y. Wu, Y. Jiang, Q. H. Liu, and S. Q. Wei, *J. Am. Chem. Soc.*, **132**, 7696 (2010).
20. S. Gomez, K. Philippot, V. Colliere, B. Chaudret, F. Senocq, and P. Lecante, *Chem. Commun.*, **19**, 1945 (2000).
21. T.-Y. Jeon, S. J. Yoo, H. Y. Park, S. K. Kim, S. Lim, D. Peck, D. H. Jung, and Y. E. Sung, *Langmuir*, **28**, 3664 (2012).
22. S. Mourdikoudis and L. M. Liz-Marzán, *Chem. Mater.*, **25**, 1465 (2013).
23. Z. Huo, C. K. Tsung, W. Y. Huang, X. F. Zhang, and P. D. Yang, *Nano Lett.*, **8**, 2041 (2008).
24. E. Koposova, A. Kisner, G. Shumilova, Y. Ermolenko, A. Offenhausser, and Y. Mourzina, *J. Phys. Chem. C*, **117**, 13944 (2013).
25. W. Haiss, N. T. K. Thanh, J. Aveyard, and D. G. Fernig, *Analyt. Chem.*, **79**, 4215 (2007).
26. A. M. Beale, M. T. T. Le, S. Hoste, and G. A. Sankar, *Solid State Sci.*, **7**, 1141 (2005).
27. G. W. Coulston, *Science*, **275**, 191 (1997).
28. J. Zeng, Y. Y. Ma, U. Jeong, and Y. N. Xia, *J. Mater. Chem.*, **20**, 2290 (2010).
29. M.-C. Daniel and D. Astruc, *Chem. Rev.*, **104**, 293 (2004).
30. B. Ahrens, P. G. Jones, and A. K. Fischer, *Europ. J. Inorg. Chem.*, **1999**, 1103 (1999).
31. A. Kumar, S. Mandal, P. R. Selvakannan, R. Pasricha, A. B. Mandale, and M. Sastry, *Langmuir*, **19**, 6277 (2003).
32. X. Lu, H. Y. Tnan, B. A. Korgel, and Y. N. Xia, *Chemistry (Weinheim an der Bergstrasse, Germany)*, **14**, 1584 (2008).